Springer

KSME

Journal of Mechanical Science and Technology 25 (2) (2011) 441~447
www.springerlink.com/content/1738-494x
DOI 10.1007/s12206-010-1206-6

Fretting damage prediction of connecting rod of marine diesel engine †

Jung Ho Son[1,*], Sung Chan Ahn[1], Jong Gug Bae[1] and Man Yeong Ha[2]

[1]*Hyundai Maritime Research Institute, Hyundai Heavy Industries Co., Ltd., Ulsan, 682-792, Korea*
[2]*School of Mechanical Engineering, Pusan National University, Pusan, 609-735, Korea*

(Manuscript Received August 27, 2010; Revised October 13, 2010; Accepted November 11, 2010)

Abstract

There is frequent fretting damage at the mating surface of a connecting rod because the connecting rod in a combustion engine is heavily loaded as well as rotated. The flexible multi-body dynamic analysis including the elasto-hydrodynamic model is introduced to calculate the actual force acting on the connecting rod that is applied to the full cyclic simulation during one cycle. The fretting possibility at the planar upper split of the marine-head type of connecting rod is predicted by the Ruiz criterion that requires three main parameters: slip, tangential and shear stress. The Ruiz criterion is more simple and useful than the prediction model based on multi-axial fatigue failure. The fretting damage prediction at the upper split of the marine diesel engine's connecting rod is compared to the actual inspection result taken after 20,000 running hours.

Keywords: Elasto-hydrodynamic analysis; Full cyclic simulation; Fretting; Ruiz criterion

1. Introduction

Fretting is a phenomenon that concerns mechanical components in contact that are designed to be fixed but undergo small relative displacements (typically 5-50 micrometers) due to fluctuating loads. The deteriorating process that reduces the fatigue properties by promoting early crack initiation is usually referred to as fretting fatigue [1].

Fretting damage begins with local adhesion between mating surfaces and progresses when adhered particles are removed from a surface. When adhered particles are removed from the surfaces, they may react with air or other corrosive environments. Affected surfaces show pits or grooves with surrounding corrosion products. A physical model of fretting is shown in Fig. 1 [2].

Surface cracks can be initiated by fretting and led to catastrophic failure after crack propagation. Under fretting conditions, fatigue strength can be reduced by as much as 50 to 70% in comparison to fatigue strength without fretting [1]. During fretting fatigue, cracks can initiate at very low stresses. The initiation of fretting fatigue cracks depends on the state of stress on the surface, particularly stresses caused by high friction.

Unfortunately, because the fretting phenomenon may be issued after more than hundreds of millions of cycles, fretting damage and fretting fatigue damage could be experienced after a long period of time. At that time, the cost to retrofit is so unpredictable that engine designers should be primarily concerned about monitoring whether fretting occurs or not.

In general, the main parameters governing fretting and fretting fatigue damage are known as contact pressure, friction coefficient and relative slip motion. The friction coefficient is related to a surface shear stress, which plays a role in the driving force that initiates cracking on the mating surface. The other primary parameter that has an effect on crack initiation and propagation is the tangential stress on the surface [1, 2].

A connecting rod is one of key components of the moving parts in internal combustion engines and continues to translate and rotate during operation. The rotating speed of a marine diesel engine is relatively low in comparison to that of an automobile engine, and its power is much higher than that of an automobile engine. Although the rotating speed of a marine diesel engine has a medium-speed range from 600 to 1,200 rpm, most of its moving parts are made of forged steel with high strength and the inertia force acting on the moving parts is not small.

The connecting rod mainly used in marine diesel engines is a marine-head type consisting of three components: conrod shaft, big-end upper and big-end lower. The bearing bush is shrink-fitted at the small-end and the bearing shell is press-fitted by tightening the big-end bolts. The conrod

† This paper was recommended for publication in revised form by Editor Dae-Eun Kim

*Corresponding author. Tel.: +82 52 202 7410, Fax.: +82 52 250 9646
E-mail address: jhson@hhi.co.kr

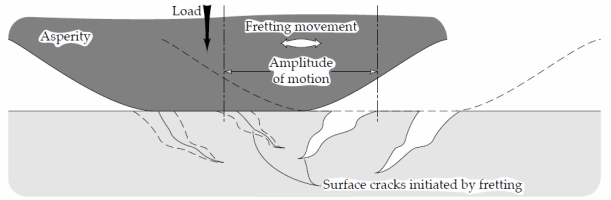

Fig. 1. Physical model of fretting.

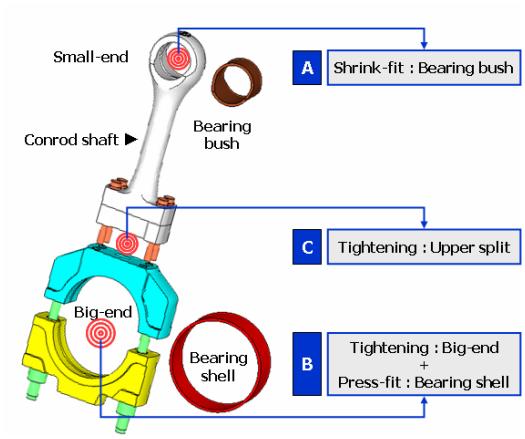

Fig. 2. Marine-head type connecting rod.

shaft with bearing bush and the big-end with bearing shell are assembled by tightening the bolt at the big-end upper and lower and the upper split (see position C in Fig. 2).

As shown in Fig. 2, several contact surfaces in the connecting rod are assembled and these contact surfaces may possibly experience fretting damage.

The connecting rod that is fractured by the fretting fatigue damage between the bearing bush and small-end is shown in Fig. 3 [3, 4]. Crack nucleation close to the oil groove caused the failure. The small-end is deformed by dynamic force acting on the bearing bush. Since the stiffnesses of the small-end and bearing bush are different, the deformation of each part is not identical in spite of the same force. The differing deformation produces a different slip that is a key contributing factor of fretting damage.

Since the connecting rod is subjected to high compressive firing force and the direction of dynamic forces acting on connecting rod is continuously changed, the fretting damage of the connecting rod can be observed more frequently than that of other components.

Recently, numerical simulation has been widely used to predict the cyclic behavior of the connecting rod, and the lubrication analysis in this simulation is also included. The lubrication film between the inner member and bearing is made and lubrication behavior, such as oil film pressure and thickness, continues to vary with the change of direction and magnitude of the dynamic loading [5]. A numerical simulation to predict the cyclic loading means the flexible multi-body dynamic analysis with the lubrication behavior. The flexible multi-body dynamic analysis model cannot

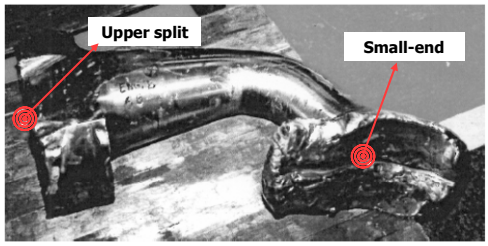

Fig. 3. Example of fretting fatigue failure.

take the stick-slip conditions into account because there is no contact surface. The lubrication analysis is an elasto-hydrodynamic lubrication (EHL) analysis to take into account the flexibility of the connecting rod.

As the results of numerical simulation, the body force and hydrodynamic pressure acting on each bearing is obtained during one engine cycle and is applied to the finite element model as boundary conditions. The finite element model with mechanical contact definition is suitable for the stick-slip simulation that can give the contact pressure and the slip on the contact surface.

The location and orientation of the fretting damage can be estimated by different multi-axial fatigue models [6]. However, most of the contact surfaces in the connecting rod are planar and the prediction of the fretting damage in the planar surface is not easy because there is no surface with locally high contact pressure. Thus, Ruiz criterion is used in order to predict the occurrence of fretting and the potential of fretting fatigue fracture. The Ruiz criterion is simple and useful in predicting the possibility of fretting damage and fretting fatigue damage [7, 8].

Fretting severity at any mating surface is quantified as fretting damage parameter (FDP). Eq. (1) is used to quantify the fretting damage related to surface separation. FDP is defined as

$$FDP = \tau \cdot \delta , \tag{1}$$

where τ is the frictional shear stress at the interface and δ is the absolute slip value in the tangential stress direction. The surface separation by fretting starts from an adhesion between the mating surfaces. After the adhesion of the mating surface, a small amount of slip results in wearing out the adhesive particle. Finally, the surface is delaminated and delamination is repeated.

The potential for fretting initiated fatigue fracture at any mating surface is quantified using the Ruiz criterion, defined as fretting fatigue damage parameter (FFDP).The fretting fatigue damage parameter is defined as follows:

$$FFDP = \sigma \cdot \tau \cdot \delta , \tag{2}$$

where σ is the tensile tangential stress on the contact surface.

In this study, results of the flexible multi-body dynamic

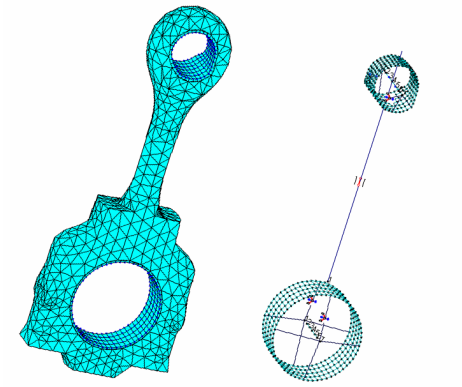

(a) Full FE model (b) Condensed model

Fig. 4. Flexible multi-body dynamic model.

simulation using EHL analysis are shown and the possibility of fretting damage at the upper split is investigated based on numerical simulation and Ruiz criterion. Prediction of fretting damage and fretting fatigue damage is compared to visual inspection after 20,000 running hours.

2. Numerical simulation

2.1 Flexible multi-body dynamic analysis

In this study, EXCITE program [9] has been used for engine dynamic analysis, including the bearing lubrication analysis [5, 10-11].

The equations of motion for the bearing and pin structure of the connecting rod are as shown in Eq. (3) and Eq. (4), respectively. The physical behavior of bearing and pin structure is described by the dynamics of elastic bodies.

$$M \cdot \ddot{y} + D \cdot \dot{y} + K \cdot y = f_{hyd} \tag{3}$$

$$M \cdot \ddot{q} = f_{hyd} + f_{ext} \tag{4}$$

The bearing is described as a kind of force element and the hydrodynamic pressure force, f_{hyd}, on each bearing is transferred and mapped to bearing and pin. M , D and K in Eq. (3) denote the mass, damping and stiffness matrix of the connecting rod, respectively. y in Eq. (3) denotes the displacement vector of connecting rod. $\ddot{y}$ and $\dot{y}$ are the acceleration and velocity vector, respectively. $\ddot{q}$ in Eq. (4) is the acceleration vector of the pin at both ends of the connecting rod. External force, f_{ext}, acts on each pin at the small-end and big-end. The oil film pressure and clearance between bearing and pin varies as time changes.

Fig. 4(a) shows the finite element model of the connecting rod, which is used to perform the flexible multi-body dynamic analysis. This finite element model consists of one big-end bearing, one small-end bearing and one connecting rod body, which are fully constrained by a multi-point constraint at each interface without the mechanical contact definition. The bearing element at both ends of connecting rod body is necessary for the elasto-hydrodynamic lubrication analysis.

A full FE model has 33,027 DOFs. The full mass and stiffness matrix of a full FE model is not suitable for efficient numerical simulation and the whole matrix size needs to be reduced. Fig. 4(b) shows the condensed model that is extracted by using a component mode synthesis method. The condensed model is generated by using Abaqus/Standard which is a particular case of the Craig-Bampton method extended to allow for large rotations and translations of the substructure. The 16 eigenmodes were extracted in the eigenfrequency extraction step at the generation level and the total number of retained DOF is 1,124.

2.2 Elasto-hydrodynamic lubrication analysis

Bearing lubrication analysis is needed to predict the oil film behavior between the bearing and pin of the connecting rod. The elasto-hydrodynamic lubrication analysis considering the stiffness and damping of the bearing and oil film is achieved by solving the extended Reynolds equation that is derived from the Navier-Stokes equation. The extended Reynolds equation can be written as

$$\frac{\partial}{\partial x}\left(\frac{1}{12\eta}h^3\theta\frac{\partial p}{\partial x}\right)+\frac{\partial}{\partial z}\left(\frac{1}{12\eta}h^3\theta\frac{\partial p}{\partial z}\right)= \theta\frac{u_1+u_2}{2}\frac{\partial h}{\partial x}+h\frac{u_1+u_2}{2}\frac{\partial \theta}{\partial x}+\frac{\partial(h\theta)}{\partial t}, \tag{5}$$

where p is the oil film pressure, θ is the fill ratio, h is the clearance height, η is the viscosity, t is time, u_1 and u_2 denote the circumferential velocity of pin and shell, *x and z* denote the coordinate in circumferential and axial direction.

Eqs. (3)-(5) are simultaneously solved. The clearance height is calculated by subtracting the displacement of the pin from the displacement of the connecting rod. Eq. (5) is used to obtain the hydrodynamic pressure distribution of the oil film in a lubrication region between bearing and pin. The lubrication pressure force which is calculated by Eq. (5) is transferred to the pin and connecting rod, respectively.

A fill ratio for mass conservation is introduced and describes the oil percentage in the gap between the bearing and pin. The fill ratio, θ, is necessary to take into account cavitation. The value of the fill ratio is from 0 to 1 in the cavitation region and is equal to 1 in the lubrication region.

If the distance between the bearing and both pins becomes very close, the clearance height, h, becomes extremely small. The extremely small clearance height turns hydrodynamic lubrication into mixed lubrication. In order to predict the pressure distribution in the mixed lubrication region, a contact pressure model is needed. The contact pressure model used in EXCITE is the Greenwood and Tripp model which has statistical values of summit roughness for asperity contact [9, 10].

The total pressure between gap clearances resulted from EHL analysis including the asperity contact model is a sum of the hydrodynamic pressure and asperity contact pressure.

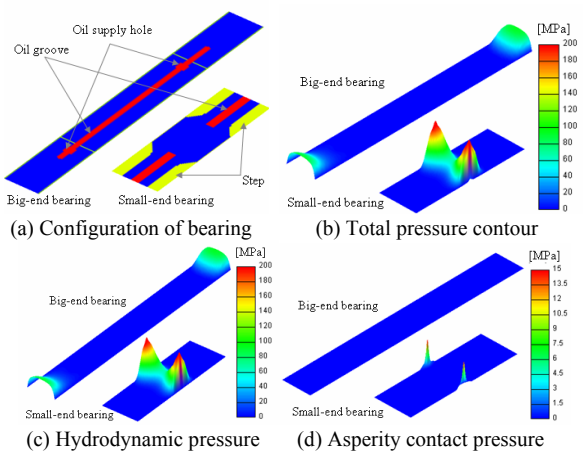

Fig. 5. Configuration of bearing and oil film pressure at CA 15°.

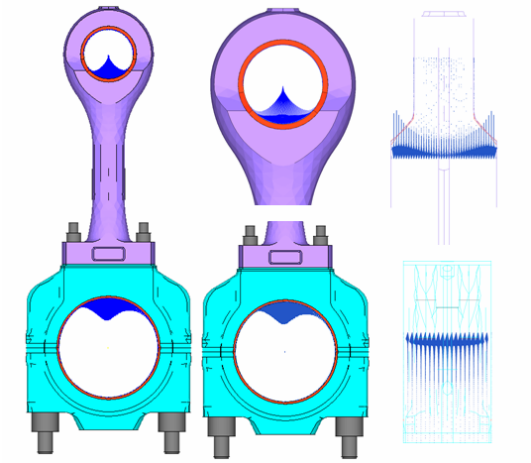

Fig. 6. Mapping of the oil film pressure on FE model.

Locally high contact pressure by elastic effect depending on surface topology between the mating surfaces is a key parameter related to bearing life due to wear.

3. Result of numerical simulation

The medium-speed diesel engine for EHL analysis is used for stationary power generation and an operating speed is 1,000 rpm. The bore and stroke of a 4-stroke engine are 250 mm and 330 mm, respectively. The maximum firing pressure is about 190 bar and the engine power per cylinder is 300 kW.

The connecting rod is of the marine-head type and the lubrication oil is supplied from the oil supply hole in the crank pin. The big-end bearing and the stepped small-end bearing are plain bearings with radial groove.

Fig. 5 shows the bearing configuration in EHL analysis and the oil film pressure contour at the crank angle (CA) of 15° when the firing in the combustion chamber occurs. CA 0° and CA 360° are TDC. BDC is CA 180° and CA 540°.

As shown in Fig. 5, total oil film pressure in the small-end bearing is higher than that in the big-end bearing and the maximum total oil film pressure in the small-end and big-end bearing are 244.7 MPa and 92.6 MPa, respectively. There is no asperity contact pressure in the big-end bearing because the piston pin is bent and the clearance between the bearing and the piston pin is very close. The maximum asperity contact pressure and the hydrodynamic pressure in the small-end bearing are 14.9 MPa and 229.8 MPa, respectively.

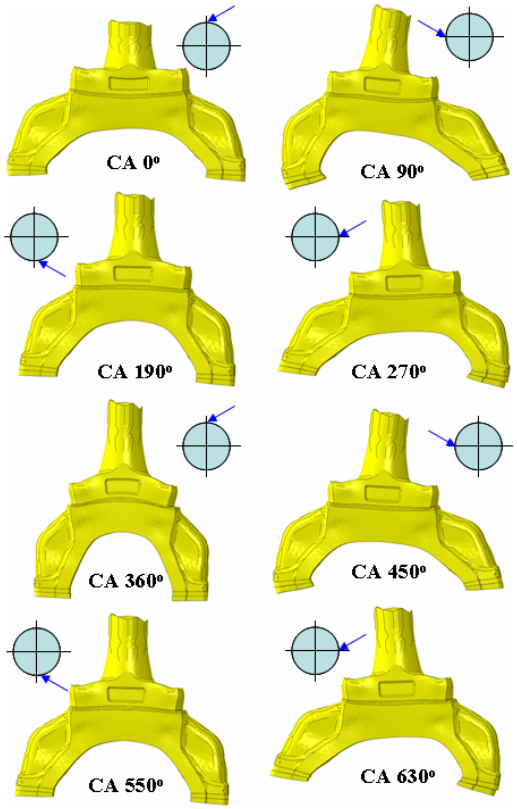

Fig. 7. Deformed shape of the connecting rod.

After EHL analysis, structural analysis is performed in order to understand the overall structural behavior of the connecting rod and more detailed interfacial characteristics at each contact surface.

After EHL analysis is performed by intervals of CA 1°, the analysis step for full cyclic simulation of the connecting rod during one cycle is divided into 47 steps, which consist of the uneven crank angle of 10° or 20°. The inertia loads and the total oil film pressure at each step are applied. Fig. 6 shows the total oil pressure distribution mapped on the FE model. The arrow indicates the nodal force, which is converted from oil film pressure.

The deformed shape of the connecting rod during one cycle is shown in Fig. 7. At TDC (CA 0°) near the firing time, the big-end is widened horizontally and is contracted vertically due to the high pressure in the combustion chamber. The upper split at this CA is deflected by the pressure force transferred from the conrod shaft. However, at another TDC

Table 1. Maximum contact pressure and tangential stress during one cycle.

Parameter	Value
Contact pressure (MPa)	260 @ CA 490°
Tangential stress (MPa)	82 @ CA 110°

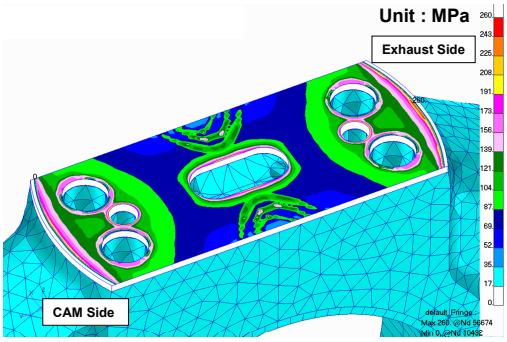

Fig. 8. Contact pressure distribution at CA 490°.

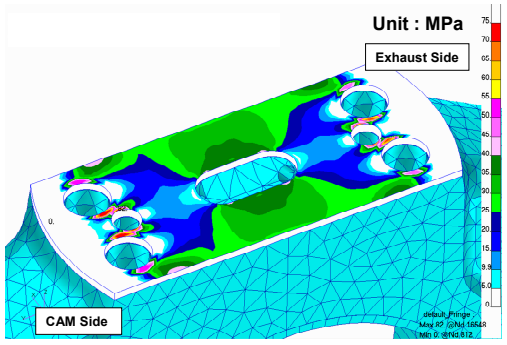

Fig. 9. Tangential stress distribution at CA 110°.

(CA 360°), the deformed shape of the big-end and the upper split is reversed due to the low cylinder pressure and the high tensile inertia force. There is almost no deformation at CA 190° and 550° as compared to the initial deformation at the assembly state due to bolt-tightening.

The big-end and upper split at TDC and BDC are deformed symmetrically in the horizontal and vertical direction, while the deformed shape of the big-end and upper split at CA 90°, 270°, 450° and 630° is distorted to one side. The deformation of the big-end and upper split changes continuously as the crankshaft rotates and firing in the combustion chamber occurs. This time-changing global deformation results in the continuous change of interfacial characteristics such as contact pressure, tangential stress, shear stress and relative slip which are Ruiz parameters.

The relative slip is related to the full cyclic simulation and the slip value at each crank angle is the cumulative slip value from assembly step to each crank angle. Therefore, the slip value at the corresponding crank angle should be the difference between the slip value at the current crank angle and the slip value at the previous crank angle. The relative slip and the absolute slip in Eq. (1) are the same.

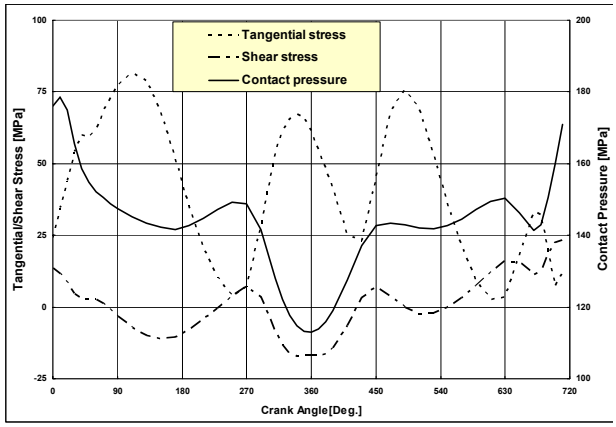

Fig. 10. Cyclic variation of contact pressure, tangential and shear stress.

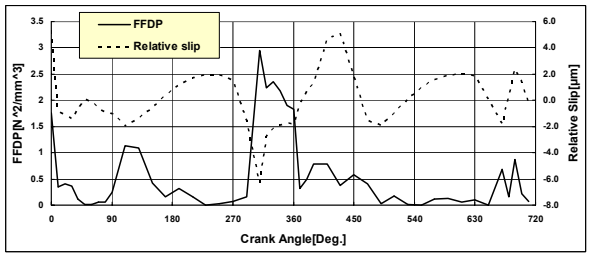

Fig. 11. Cyclic variation of relative slip and FFDP.

4. Prediction of fretting and fretting fatigue damage

Cyclic variation of Ruiz parameters is needed to predict a possibility of fretting damage and fretting fatigue damage. The maximum value of each parameter is found from full cyclic simulation during one cycle and occurs at different times. Maximum contact pressure and tangential stress in the upper split surface during one cycle are shown in Table 1. Maximum contact pressure during one cycle is 260 MPa at CA 490° and occurs at the edge of both sides, as shown in Fig. 8. Contact pressure is much higher at the edge and around the bolted area than at the planar surface. As shown in Fig. 9, maximum tangential stress during one cycle is 82 MPa at CA 110° and occurs at the bolted area where the contact pressure is high and the structural constraint is strong.

Figs. 10-11 show the cyclic variation of the contact pressure, the tangential stress, the shear stress, the relative slip and FFDP at the position where the fretting fatigue damage is the greatest. The position of the maximum fretting fatigue damage is the same as that of the greatest tangential stress. This means that crack initiation and propagation by fretting are dominated by the tangential stress when the contact pressure is high.

The change of the pressure in the combustion chamber is related to the cyclic variation of the contact pressure at the upper split surface. The value of the contact pressure peaks as the firing in the combustion chamber occurs. The contact

Table 2. Ruiz parameters and FFDP at CA 310°.

Parameter	Value
Tangential stress (MPa)	54.3
Relative slip (μm)	-6.33
Shear stress (MPa)	-8.6
Contact pressure (MPa)	127.9
FFDP (N^2/mm^3)	2.95

pressure has a peak and a valley during one cycle. The tangential stress and shear stress vary more frequently with changes of the rotating direction and magnitude. Changes in the tangential stress and shear stress are closely related to the inertia force rather than the pressure force.

The cyclic variation of relative slip and FFDP is shown in Fig. 11. The relative slip is bigger at CA 0°, CA 310° and CA 430°. The reason for the large relative slip at CA 0° is the sudden change experienced by acting on the pressure force after the assembly step. Therefore, the FFDP value at CA 0° is unrealistic due to a numerical technique. On the basis of CA 360°, the relative slip suddenly changes from negative to positive, and this tendency has a dominant effect on the fretting fatigue damage as shown in Fig. 11. The FFDP is greatest at CA 310°, and the Ruiz parameters and FFDP at this time are shown in Table 2. The contact pressure and tangential stress at CA 310° are smaller in comparison to the maximum contact pressure and tangential stress at all points during one cycle, as shown in Table 1. The greater tangential stress and slip increase the possibility of fretting fatigue damage.

The FDP and FFDP distribution calculated on the upper split are shown in Fig. 12. As compared to Fig. 8, both ends of the cam and exhaust side and the center area in the split surface show high contact pressure, but FDP and FFDP are close to zero. This means that the contact pressure at the mating surface is not a good parameter to predict the fretting damage and fretting fatigue damage.

A photograph taken after 20,000 running hours shows a slight pitting mark on the exhaust side that is highlighted by the yellow dotted line. The amount of slip in this area is relatively bigger than on other planar surfaces except around the bolting hole as shown in Fig. 13. Fig. 13 shows the slip amplitude, which is half the difference between maximum slip and minimum slip. The cumulative FDP value at the pitting area is below 0.11 N/mm and the peak cumulative FDP value is 0.8 N/mm. The difference of the FDP predicted between the cam side and exhaust side is very small. However, it was found that the fretting severity on the exhaust side is a little higher than in the cam side after overhauling and inspection, as shown in the left photograph in Fig. 12.

The maximum cumulative FFDP during one cycle is 27.0 N^2/mm^3 and there is no crack at the maximum cumulative FFDP. Therefore, the threshold FFDP value for crack initiation by fretting fatigue damage is regarded to be much higher.

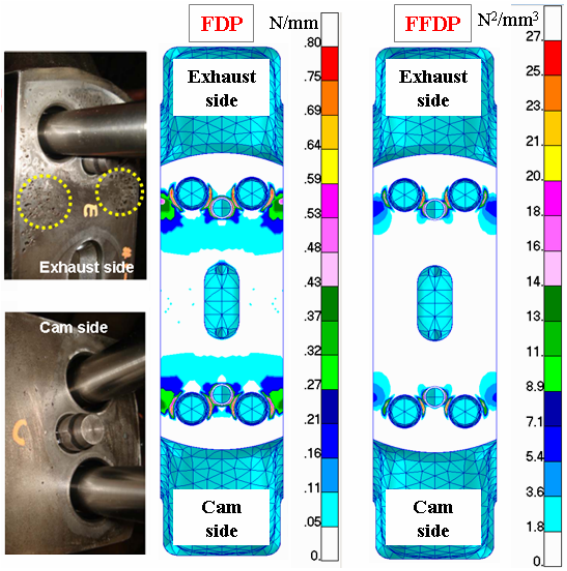

Fig. 12. Cumulative FDP and FFDP distribution.

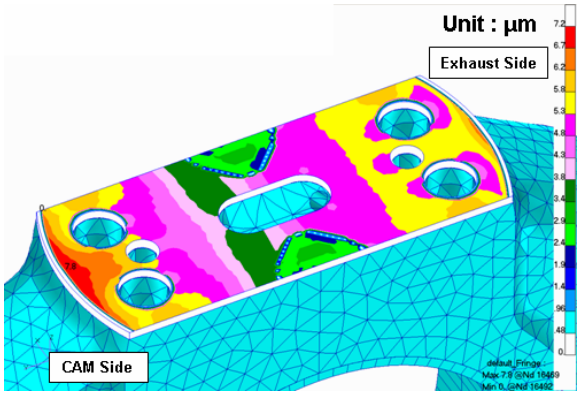

Fig. 13. Slip amplitude distribution.

5. Conclusions

Multi-body flexible dynamic analysis with an EHL model and full cyclic simulation during one cycle are performed to predict the realistic structural behavior of the connecting rod for marine diesel engines. The marine–head type connecting rod with three main split surfaces always has the possibility of fretting damage and fretting fatigue damage. The Ruiz criterion that is adapted to predict the fretting severity is very practical from the viewpoint of its parameters and is suitable for predicting the fretting damage in the planar contact surface at the upper split in the connecting rod.

Acknowledgment

This work was supported by the National Research Foundation of Korea (NRF) grant funded by the Korean Government

(No.K20702001648-10E0100-07010).

References

[1] S. J. Shaffer and W. A. Glaeser, *ASM Handbook : Fatigue and Fracture (fretting fatigue)*, ASM International, 19 (1996) 321-330.

[2] G. W. Stachowiak and A. W. Batchelor, *Engineering Tribology*, Butterworth Heinemann (2001).

[3] R. Rabb, Fatigue failure of a connecting rod fatigue failure of a connecting rod, *Engineering Failure Analysis*, 3 (1) (1996) 13-28.

[4] R. Rabb, P. Hautala and A. Lehtovaara, Fretting fatigue in diesel engineering, *CIMAC World Congress 2007*, Vienna, Paper No. 76 (2007).

[5] B. J. Kim and K. W. Kim, Thermo-elastohydrodynamic analysis of connecting rod bearing in internal combustion engine, *ASME J. Tribol.* 123 (3) (2001) 444-454.

[6] M. Fooks, J. Harrison, D. Bell and H. Govett, A study considering the influence of the connecting rod structure on big end bearing performance, *CIMAC World Congress 2007*, Vienna, Paper No. 138 (2007).

[7] J. Vidner and E. Leidich, Enhanced Ruiz criterion for the evaluation of crack initiation in contact subjected to fretting fatigue, *Int. J. Fatigue*, 29 (2007) 2040-2049.

[8] D. Merritt and G. Zhu, The prediction of connecting rod fretting and fretting initiated fatigue fracture, *SAE Technical Paper 2004-01-3015 (*2004).

[9] AVL LIST GmbH, *Users Guide : EXCITE Power Unit*, 7.0.2 (2007).

[10] V. Fridman, I. Piraner and C. Musolff, Analysis based solutions for engine bearing related problems, *CIMAC World Congress 2007*, Vienna, Paper No. 281 (2007).

[11] A. Francisco, A. Fatu and D. Bonneau, Using design of experiments to analyze the connecting rod big-end bearing behavior, *ASME J. Tribol.* 131 (1) (2009).

Jung Ho Son received his B.S and M.S. in Mechanical Engineering from Pusan National University, Pusan, Korea, in 1993 and 1995. At present, he is a Ph.D. candidate at the school of Mechanical Engineering at Pusan National University and a principal researcher in Hyundai Maritime Research Institute, Hyundai Heavy Industries Co., Ltd. His research interests focus on the durability of marine diesel and gas engine.